



Published in final edited form as:

Nat Genet. 2008 December ; 40(12): 1454–1460. doi:10.1038/ng.267.

The Forkhead protein, FoxJ1, specifies node-like cilia in *Xenopus* and Zebrafish embryos

Jennifer Stubbs, Isao Oishi, Juan Carlos Izpisua Belmonte, and Chris Kintner¹

The Salk Institute for Biological Studies, Post Office Box 85800, San Diego, California 92186-5800

Abstract

Ciliated cells that produce a leftward fluid flow have been proposed to mediate left-right patterning in many vertebrate embryos. The cilia on these cells combine features of primary sensory and motile cilia, but how this cilia subtype is specified is unknown. We address this issue by analyzing the *Xenopus* and Zebrafish homologs of FoxJ1, a forkhead transcription factor necessary for ciliogenesis in multi-ciliate cells of the mouse. We show that the cilia that underlie left-right patterning on the *Xenopus* gastrocoel roof plate (GRP) and Zebrafish Kupffer's vesicle (KV) are severely shortened or fail to form in *FoxJ1* morphants. We also show that misexpressing XFoxJ1 is sufficient to induce ectopic GRP-like cilia formation in frog embryos. Microarray analysis indicates that XFoxJ1 induces the formation of cilia by upregulating the expression of motile cilia genes. These results indicate that FoxJ1 is a critical determinant in specifying cilia used in left-right patterning.

Introduction

Cilia are microtubule-based organelles that project hair-like from the surface of cells. Cilia can be generally subdivided into motile and sensory subtypes that differ markedly in structure and function¹. Sensory cilia are typically short in length, lack structural features such as the central pair and dynein arms but play important roles in detecting chemical, or mechanical stimuli as an extension of the cell surface. One hallmark of sensory cilia is that they invariably form as a single cilium on non-dividing cells when the paired centrioles docks at the cell surface, allowing the mother centriole to form a basal body and initiate ciliogenesis, apparently as a default pathway². By contrast, motile cilia that form on epithelial cells within such tissues as the ependyma or the respiratory airways are specialized to produce fluid flow¹. Cilia of the motile subtype have a 9+2 axonemal structure, use dynein arms to produce a whip-like power stroke and likely have other structural features required for oriented flow. In addition, each flow-producing cell typically projects hundreds of cilia, requiring mechanisms not likely to be initiated in cells with sensory cilia, for example those that mediate acentriolar duplication.

Users may view, print, copy, and download text and data-mine the content in such documents, for the purposes of academic research, subject always to the full Conditions of use:http://www.nature.com/authors/editorial_policies/license.html#terms

¹Communicating Author: Kintner@salk.edu.

Accession Numbers: Microarray data is deposited at NCBI (Accession number GSE12613)

In the mouse, a genetic distinction has been made between cells that form sensory and motile cilia based on the analysis of the forkhead protein, FoxJ1, also known as HFH-4³. Mouse FoxJ1, a transcriptional activator, is expressed in multi-ciliate cells within the respiratory tract, oviduct and choroid plexus⁴⁻⁶. In mice null for FoxJ1 by targeted deletion, multi-ciliate cells still duplicate their centrioles but fail to properly dock them at the apical surface and extend cilia⁷⁻⁹. By contrast, loss of FoxJ1 does not appear to disrupt the formation of sensory cilia, such as those present in olfactory epithelium or in the kidney^{10,11}. Thus, FoxJ1 is required for cells to form motile but not sensory cilia.

A third subtype of cilia found in the mouse is located on cells at the embryonic node, a structure present in the early embryo that underlies the breaking of left-right symmetry¹². Node cilia beat with a clockwise rotational motion, thereby creating a leftward flow of extracellular fluid over the node surface¹³. Despite their functional resemblance to the multi-ciliate cells that produce fluid flow, node cells only form a single cilium, a hallmark of sensory cilia. Moreover, node cilia in the mouse are thought to lack a central pair, thus resembling both motile and sensory cilia in axonemal structure¹⁴. FoxJ1 null mice have randomized left-right asymmetry, indicating a defect in node cilia, but monociliated cells at the embryonic node are still present^{10,11,15}. Thus, it is not clear whether the formation of node cilia involve pathways used by motile or sensory cilia and what role FoxJ1 might have in their formation.

In *Xenopus*¹⁶ and fish^{17,18}, embryonic structures related to the mouse node have cells with monocilia that also produce a leftward flow, namely the gastrocoel roof plate (GRP) and Kupffer's vesicle (KV), respectively. We therefore examined the role of FoxJ1 in the formation of ciliated cells in these structures, asking whether FoxJ1 function is required for these cells to mediate left-right patterning, and if so how. Our results indicate that FoxJ1 is both necessary and sufficient to drive the formation of node-like cilia in embryonic epithelia, suggesting that this cilia subtype forms in cells using a similar genetic pathway used in multi-ciliate cells.

Results

FoxJ1 in left-right patterning

FoxJ1 null mice have left-right patterning defects despite forming node cilia^{10,11,15}. To determine whether this holds true for other vertebrate species, we initially examined Zebrafish embryos, where monociliated cells within Kupffer's vesicle (KV) produce a directional flow required for the establishment of left-right asymmetry¹⁷. *ZFoxJ1* RNA is expressed in KV as early as stage 6ss, and later in the developing pronephric duct where motile, multi-ciliate cells form (Supplementary Fig. 1A,B). To determine the function of *ZFoxJ1* in cells of KV, Zebrafish embryos were injected with a morpholino designed to block the translation of *ZFoxJ1* RNA (*ZFoxJ1*^{MO}). *ZFoxJ1* morphants develop with severe defects in left-right heart jogging, consistent with a defect in KV cilia function (Supplementary Fig. 1C-E)^{17,19}. When *ZFoxJ1* morphants were stained with the acetylated tubulin antibody that stains cilia, KV forms (Fig. 1A,B) but many of the cells lack cilia (Fig. 1 C,D) and the remaining cilia are shortened (Fig. 1I). Thus, morpholino knock down of *ZFoxJ1* function causes defects in left-right patterning (Supplementary Fig. 1E), a two-fold

decrease in the number of KV cilia (Fig. 1C,D), and a 3.5-fold decrease in the average length of KV cilia (Fig. 1I).

In *Xenopus* embryos, monociliated cells located on the gastrocoel roof plate (GRP) produce a directional flow, thus acting as the equivalent of KV in left-right patterning¹⁶. The GRP arises from the superficial layer of the dorsal involuting marginal zone (DIMZ), which expresses *XFoxJ1* transiently as it involutes over the blastopore lip to form the GRP during gastrulation (Supplementary Fig. 2A-D)²⁰. To examine the function of *XFoxJ1* in these cells, *Xenopus* embryos were injected at the two-cell stage with morpholinos designed to block either the translation (*XFoxJ1*-MO^{ATG}), or splicing (*XFoxJ1*-MO^{SPL}) of *XFoxJ1* RNA. Morphants were fixed at stage 17 and analyzed by staining with antibodies directed against ZO-1 and acetylated tubulin to label cell junctions and cilia, respectively (Fig. 1E-H)). Injecting embryos with either *XFoxJ1* morpholino, or a mixture of both morpholinos, but not a control morpholino, reduced the percentage of GRP cells that extend cilia by two-fold and the length of GRP cilia by four-fold (Fig. 1E-I, Supplementary Fig. 3A-D). In addition, both phenotypes were completely rescued by co-injecting a synthetic flag-tagged form of *XFoxJ1* RNA lacking sequences recognized by either morpholino (Supplementary Fig. 3E-G). Thus, the cilia on the Zebrafish KV or on the *Xenopus* GRP are lost and severely shortened when *FoxJ1* function is reduced.

FoxJ1 is required for ciliogenesis in *Xenopus* multi-ciliate cells

The role of *FoxJ1* in the formation of node-like cilia appears to differ between Zebrafish/*Xenopus* and the mouse. We therefore extended our analysis of *XFoxJ1* to multi-ciliate cells to determine whether in this context, the function of *FoxJ1* is conserved. The multi-ciliate cells that form in the *Xenopus* larval skin after stage 26 closely resemble those found in the mouse respiratory tract and express *XFoxJ1* (Supplementary Fig. 2E-G), and thus allow one to directly compare *FoxJ1* function in the formation of motile cilia in different species.

Injecting either *XFoxJ1* morpholino, but not a control morpholino, produced a dose-dependent defect in skin cilia formation: at a lower dose, cilia formed, but were reduced in number and often shortened in length while at higher doses, most cilia were lost in the skin except for an occasional stumpy cilium (Fig. 2A-B, Supplementary Fig. 4). Ciliated cells can be distinguished from other cell types in the skin based on their characteristic morphology and spacing pattern²¹. Based on these criteria, ciliated cells were still present at their normal density in embryos injected with *XFoxJ1*^{MO} even as cilia were completely lost (data not shown). In addition, ciliogenesis in multi-ciliate cells was fully restored in *XFoxJ1* morphants by injecting a flagged-tagged *XFoxJ1* (Supplementary Fig. 5), indicating that the cilia phenotypes in *XFoxJ1* morphants were specific. Thus, these results indicate that *XFoxJ1* plays a conserved role in the ciliogenesis of multi-ciliate cells.

In the mouse, *FoxJ1* has been proposed to activate gene expression required to dock basal bodies at the apical surface, an obligatory step in the process of ciliogenesis⁷⁻⁹. To determine whether this is also true in *Xenopus* ciliated cells, basal bodies were labeled in the *FoxJ1* morphants using a centrin2-GFP fusion protein and visualized using confocal microscopy (Fig. 2C-D)²². Indeed, the number of basal bodies localized apically per cell was reduced in *FoxJ1* morphants relative to control morphants by about 30% (167 ± 34

versus 112 ± 28 , $P < .005$). Since this assay may overestimate the number of basal bodies intimately docked to the apical surface, we examined the location of basal bodies in ciliated cells in relation to the actin-rich apical cortex that can be stained with Rhodamine-Phalloidin^{22,23} (Fig. 2E). In controls, the centrin-labeled basal bodies are embedded in this apical actin network, presumably anchoring them for ciliogenesis (Fig. 2E). Strikingly, in FoxJ1 morphants, apical actin staining was largely lost, while cortical actin labeling at cell-cell contacts was unaffected (Fig. 2E), and the centrin2-labeled basal bodies were located below the residual apical actin rather than co-mingled as in the controls (Fig. 2E, panel Z). These observations parallel those in the mouse, suggesting that XFoxJ1 plays a conserved role in ciliogenesis in multi-ciliate cells, presumably by activating genes required for basal body docking and ciliogenesis.

XFoxJ1 expression induces cilia in ectopic location

Previous experiments in which FoxJ1 was mis-expressed in cultured cells or transgenic mice indicated that FoxJ1 is not sufficient to induce multi-ciliate cell differentiation, in line with the idea that FoxJ1 acts relatively late in these cells to promote ciliogenesis²⁴. We were therefore surprised to find that when *XFoxJ1* RNA was injected into embryos to rescue the morpholino phenotypes, ectopic cilia readily formed in a number of locations. For example, when *XFoxJ1* RNA was targeted to the marginal zone to rescue cilia formation on the GRP, ectopic cilia also formed at the midline more anteriorly, as well as on the lateral, endodermal epithelial crest that migrates to cover the GRP at later stages (Supplementary Fig. 6A-B). Similarly, when *XFoxJ1* RNA was targeted to the ectoderm, cilia ectopically formed on cells within the superficial epithelium (Fig. 3A-D). In both locations, the ectopic cilia induced by XFoxJ1 were similar in length to those on the GRP (Fig. 3D, Supplementary Figs. 3 and 6B) and formed on cells that are not normally ciliated. We also used Wilson explants to visualize primary cilia that form on mesenchymal cells within the dorsal mesoderm (Supplementary Fig. 7A). Primary cilia on mesodermal cells still form in XFoxJ1 morphants (Supplementary Fig. 7C) but are replaced by longer cilia in embryos injected with *XFoxJ1* RNA (Supplementary Fig. 7B,D). Thus, ectopic expression of *XFoxJ1* in embryonic cells derived from all three germ layers can induce cilia formation de novo, and/or alter the formation of cilia subtype.

FoxJ1 induced cilia are node-like

Based on length, the cilia induced by *XFoxJ1* resemble those on the GRP ($\sim 5\mu\text{m}$)¹⁶, rather than primary cilia ($\sim 1\mu\text{m}$) or those on multi-ciliate cells ($\sim 11\mu\text{m}$). To assess this resemblance further, we further analyzed the ectopic cilia induced by FoxJ1, focusing on those that arise in a superficial layer of the ectoderm. First, we analyzed the ectopic cilia in light of the finding that Notch signaling negatively regulates the differentiation of multi-ciliate cells²⁵⁻²⁷ but not the formation of cells with node-like cilia. Thus, expressing an activated form of the Notch receptor, ICD, in *Xenopus* embryos by RNA injection, leads to a complete loss of multi-ciliate cells in the skin (Fig. 3E)²⁵, but not the ciliated cells on the GRP (Supplementary Fig. 6C-D). In embryos injected with both *XFoxJ1* and *ICD* RNA, multi-ciliate cells still failed to form (Fig. 3E) while ectopic cilia resembling those on the GRP were still induced (Fig. 3F). The ectopic cilia induced by FoxJ1, like those on the GRP, are therefore insensitive to Notch signaling.

Second, we asked whether the cilia induced by FoxJ1 resemble motile primary cilia by characterizing their axonemal structure using transmission electron microscopy (TEM). Motile cilia invariably have dynein arms emanating from each of the nine outer microtubule doublets, and can be 9+0, 9+2, or even 9+4²⁸. When cilia induced by FoxJ1 were analyzed by TEM, they contained a central doublet (9+2), and dynein arms (Fig. 3H), indicating that these cilia are of the motile subtype and virtually identical in structure to the cilia formed by multi-ciliate cells in the skin (Fig. 3G).

Finally, we characterized the beat pattern of ectopic cilia induced by XFoxJ1 using high-speed microscopy. Some of the FoxJ1-induced cilia produced a clockwise rotational motion like GRP cilia (Supplementary Movie 1), others produced a more whip-like motion (Supplementary Movie 2), while others produced a hybrid between the two. In addition, the beat frequency of the ectopic cilia ranged from 12-37Hz with an average of 23 ± 8 Hz, thus corresponding on average to those at the GRP¹⁶. The cilium with a whip-like pattern tended to be longer and slower, while those with a rotational pattern tended to be shorter and faster. The relatively wide variation in beat frequency and beat pattern of ectopic cilia could be due to the fact that the level and timing of *XFoxJ1* misexpression do not fully mimic the pattern of *XFoxJ1* expression that normally occur in GRP cells. Together these data suggest that the ectopic cilia induced by XFoxJ1 are similar in cilia subtype as those used to generate leftward flow.

High levels of FoxJ1 misexpression induces bi-ciliated cells

In embryos injected with higher levels of *XFoxJ1* RNA, a significant fraction of cells formed two ectopic cilia rather than a monocilium (Fig. 4B,E). To induce two cilia, XFoxJ1 must promote centriole duplication or split the centriole pair so that both mother and daughter centrioles mature as basal bodies and initiate ciliogenesis. To examine this phenotype further, we visualized centrioles in *XFoxJ1* RNA injected embryos using an antibody directed against γ -tubulin. In an uninjected epithelial cell, centriole-pairs labeled with the γ -tubulin antibody tend to be located in a basolateral position (Fig. 4A). By contrast, in *XFoxJ1* RNA injected embryos, these structures relocated to a central apical position where one or two ectopic cilium formed (Fig. 4B). In some cases, these structures remained paired and the cell formed only one cilia. In about 50% of the cells, however, the centrioles were split (Fig. 4F), resulting in some cases in two cilia per cell. Together these results indicate that ectopic expression of *XFoxJ1* not only induces apical docking of centrioles as basal bodies, but also has a profound effect on basal body formation in ways that allow a cell to form two cilia.

We next asked whether the bi-ciliated cells induced by XFoxJ1 are normally present on the GRP (Fig. 4C,D). Indeed, in uninjected embryos, 14% of the cells on the GRP project two cilia based on acetylated tubulin staining (Fig. 4C, E). Based on γ -tubulin staining, approximately 40% of cells in the GRP contained two well-separated centrioles (Fig. 4D, F). Thus, bi-ciliate cells normally arise within the GRP presumably in response to higher levels of *FoxJ1* expression.

FoxJ1 activates gene expression encoding components of motile cilia

Based on the proposed function of FoxJ1 in multi-ciliate cells in the mouse, one model is that FoxJ1 induces node-like cilia by simply promoting the apical docking of centrioles where they form basal bodies and initiate ciliogenesis. An alternative model, however, is that FoxJ1 upregulates genes that are not only required for basal body docking, but also those required for cilia motility. To distinguish between these two models, we used Affymetrix microarrays to survey the genes that are induced ectopically by XFoxJ1 when it induces ectopic cilia formation.

To perform this analysis we exploited that fact that XFoxJ1 can still induce the formation of ectopic cilia while the formation of multi-ciliate cells is blocked by expressing an activated form of the Notch receptor (ICD) (Fig. 3E)²⁵. We therefore prepared RNA from cultured ectoderm that expresses both *ICD* and *XFoxJ1*, as well as RNA from ectoderm injected with just *ICD* RNA. The expression levels of RNAs were then compared between these two samples, initially focusing on those that were elevated by at least 10-fold by XFoxJ1 in an ICD background (Table 1 Supplementary Data).

Of the approximately 100 genes upregulated 10-fold by XFoxJ1, a third encode the *Xenopus* homologs of proteins found in a ciliome database assembled using a survey of bioinformatics, genomics and proteomics studies²⁹, including many proteins found in axonemal structures exclusive to motile cilia. For example, XFoxJ1 induced genes whose products comprise the dynein arms, including heavy chain subunits (DNAH9 and DNAH8), an intermediate chain subunit (DNAI1) a WD40 repeat protein potentially involved in dynein arm assembly, isoforms of adenylate kinase, (AK5 and AK7), a dynein light chain (Tctex-1), and a dynein associated protein (roadblock) related to LC7 in *Chlamydomonas*. XFoxJ1 also induced at least one component of the central pair complex, Spag6, and various radial spoke proteins, including RSHL2, RSHL3, and radial spoke protein 44. XFoxJ1 induced the expression of four tektin isoforms, including one that is required for the function of motile cilia in the mouse. Thus, when FoxJ1 induces the formation of node-like cilia, it apparently does so by inducing the expression of genes required for cilia motility

Validation of FoxJ1 induced gene expression

To validate the results from the microarray analysis, we examined the expression of several genes on the FoxJ1 upregulated list, focusing on three likely to be critical for cilia motility based on mouse mutants, namely *PF16*, *Tektin-t* and *LR-dynein*³⁰⁻³². When examined by whole mount, in situ hybridization, all three genes are expressed in the multi-ciliate cells in the skin, are lost when multi-ciliate cells are eliminated by expressing ICD, or when ciliogenesis is blocked in the multi-ciliate cells by injecting the XFoxJ1^{MO} (Data not shown, Supplementary Fig. 8). Thus, all three genes are expressed in multi-ciliate cells in a FoxJ1-dependent manner. All three genes are expressed in the GRP (Fig. 5A-C), and are markedly upregulated ectopically in embryos misexpressing FoxJ1 (Fig. 5A-C, Supplementary Figs. 7E-G, and 8). To confirm these observations quantitatively real-time PCR was used to measure RNA levels of *PF16*, *Tektin-t* and *LR-dynein* when the embryonic epithelium is explanted on fibronectin-coated glass (Fig. 5D). In explants injected with *ICD* RNA alone, the expression levels of these three cilia genes dropped approximately 8-fold relative to

control, inline with the idea that these genes are expressed in multi-ciliate cells. Moreover, in explants that express both FoxJ1 and ICD, the levels of RNA encoding these three cilia proteins increased approximately 5-10 fold over the levels found in control larval skin and 50 fold or more relative to ICD injected samples. Thus, these results indicate that when *XFoxJ1* induces node-like cilia in ectopic locations, it upregulates the expression of genes involved in cilia motility.

Discussion

Specification of cilia subtype is a critical aspect of cell type differentiation but the developmental mechanisms involved remain poorly understood. Many cell types form primary sensory cilia, and the formation of this cilia subtype can be triggered when certain centriole-associated proteins are downregulated². The implication is that most cells constitutively produce the proteins required for sensory cilia formation, and will do so once centriole function is no longer required during the cell cycle. Conversely, the formation of motile cilia during the differentiation of multi-ciliate cells is likely to involve a more elaborate genetic program, part of which has been shown in the mouse to involve FoxJ1. Here we provide evidence that the formation of node-like cilia on cells not only requires FoxJ1 but that FoxJ1 is sufficient to induce this pathway of cilia subtype differentiation in many embryonic cell types. Our results reveal an unexpected central role of FoxJ1 in activating gene expression required for the formation of motile node-like cilia, a role likely relevant to its function in the differentiation of multi-ciliate cells.

In the mouse, a null mutation in FoxJ1 establishes its role in the differentiation of multi-ciliate cells³. Ciliated cells still form and undergo centriole duplication, but fail to dock centrioles as basal bodies at the apical surface⁹. The multi-ciliate cells in the *Xenopus* skin are indistinguishable from those affected in the FoxJ1 mutant mouse. Indeed, when XFoxJ1 activity is inhibited in *Xenopus* embryos using morpholinos, the ciliated cells in the skin are still present, centriole duplication occurs, but basal body docking is disrupted and ciliogenesis fails. These phenotypes indicate that FoxJ1 plays a conserved role in the differentiation of multi-ciliate cells, by promoting a relatively late step in ciliogenesis.

The left-right axis is randomized in FoxJ1 mouse mutants, suggesting defects in node cilia, but monociliated cells at the node are still present. This observation raises a paradox since one would expect that FoxJ1 would be required for basal body docking both in multi-ciliate and node cells. By contrast to the mouse, when FoxJ1 is inhibited in Zebrafish and *Xenopus* embryos using morpholinos, ciliated cells and cilia length are markedly reduced in KV and GRP, respectively. In addition, ectopic expression of XFoxJ1 in *Xenopus* induces ectopic cilia, with properties similar to GRP cilia, to form in several locations. Finally, XFoxJ1 induces the formation of node-like cilia by activating a large number of genes that are associated with motile cilia. These results strongly indicate that FoxJ1 specifies the formation of node-like cilia, suggesting that this cilia subtype arises using the same genetic program that drives ciliogenesis in multi-ciliate cells.

What might account for the fact that cilia are lost in the *Xenopus* GRP and Zebrafish KV in FoxJ1 morphants while cells at the embryonic node in FoxJ1 null mice are still ciliated

despite left-right axis randomization¹⁵? One explanation is that in *Xenopus*/*Zebrafish* the formation of node-like cilia is more dependent on FoxJ1 while in mouse redundant factors may come into play. However, another explanation is based on the observation that mouse node contains two populations of monociliated cells³³, one of which is centrally located, *lrd* positive, and extends a motile cilium while the other is more peripheral, *lrd* negative, and extends a sensory cilium. Thus, all node cells can conceivably form sensory cilia, thus masking the loss of the motile cilia subtype in FoxJ1 mutants. By contrast, sensory cilia appear to be less prevalent in either the *Zebrafish* KV or the frog GRP, perhaps making the loss of the motile node-like cilia more obvious. In this view, FoxJ1 plays a conserved role in specifying the motile, node-like cilia in vertebrates, while the prevalence of sensory cilia among cells that mediate left-right patterning is more variable.

How might FoxJ1 specify node-cilia differentiation? As predicted by the null-phenotype in multi-ciliate cells, one downstream consequence of FoxJ1 misexpression is the apical docking of basal bodies. Additionally, FoxJ1 promotes the formation of bi-ciliate cells, suggesting that it activates genes whose products split the centriole pair and promote the maturation of the daughter centriole into a basal body. Finally, FoxJ1 activates the expression of a relatively large panel of genes that encode components exclusive to motile cilia, including dynein arms, central pair, and radial spokes. Thus, FoxJ1 appears to be sufficient to activate the gene expression required to convert a non-ciliated cell into one with the flow producing properties required for left-right patterning.

The ability of FoxJ1 to induce ectopic cilia formation is not universal, and even at the highest concentrations tested not all cells were ciliated. This observation may explain why ectopic FoxJ1 does not noticeably reduce cell division, presumably because other factors determine whether cells form cilia in response of FoxJ1. One potential regulatory factor is the centriole-associated protein CP110, which has been proposed to regulate the formation of primary sensory cilia². Indeed, when XCP110 is overexpressed in *Xenopus* embryos, it inhibits ciliogenesis both in multi-ciliate cells as well as those induced by ectopic FoxJ1, suggesting that it may also regulate motile cilia formation (J. Stubbs, unpublished observation).

Based on these results, we propose a model for how different cilia subtypes are specified in development (Fig. 6). In this model, FoxJ1 is sufficient to activate gene expression required for the formation of motile cilia, which are genetically distinct from primary cilia. Expression of FoxJ1 can specify node-like cilia as well as a distinct bi-ciliate cell whose function and prevalence warrants further investigation. Finally, we propose that FoxJ1 is also required to activate the motile cilia pathway in multi-ciliate cells, where additional unknown factors are required to promote the early steps of differentiation, including the ones that drive the process of centriole duplication. In sum, while sensory cilia have been proposed to form via a default pathway, those used to produce fluid flow during left-right patterning and in multi-ciliate cells require a genetic program driven by FoxJ1. It will be of interest to determine whether the cilia that form using a FoxJ1-dependent pathway share other properties, including how their orientation is determined for directed flow³⁴.

Materials and Methods

Xenopus laevis fertilizations, microinjections and embryo culture

Xenopus embryos were obtained by *in vitro* fertilization using standard protocols³⁵. Embryos were injected at the two-cell stage with capped, synthetic mRNAs (1-5 ng) that encode centrin2 fused to GFP (centrin2-GFP)²², membrane-localized mRFP as a control or lineage tracer²¹, or the intracellular domain of Notch (ICD)³⁶. *XFoxJ1* RNAs encoded the full-length protein, or a protein where a flag-tag was added to the amino terminus, changing the start of translation. Morpholinos (Genetools) directed against XFoxJ1 RNA targeted the initiation codon (XFoxJ1-MO^{ATG}), or the first splice acceptor site at the junction between intron1 and exon2 (XFoxJ1-MO^{SPL}) (Supplementary Table 2)^{37,38}. Efficacy of the splicing morpholino was assayed using RT-PCR (Supplementary Fig. 9). Unless indicated otherwise, embryos were injected with 30ng of the XFoxJ1-MO^{ATG}, 75ng of the XFoxJ1-MO^{SPL}, the same dose of the two XFoxJ1 morpholinos mixed together, or 75ng of the control morpholino.

In-situ Hybridization and Immunofluorescence

Whole mount, *in situ* hybridizations were performed as described³⁹. Embryos were fixed for immunohistochemistry in 4% paraformaldehyde in Phosphate Buffered Saline (PBS) for 1 hour on ice (*Xenopus*) or overnight at 4°C (Zebrafish), followed by dehydration in 100% ethanol. Dorsal explants were placed underneath a glass coverslip just prior to fixation, in order to flatten out the curvature of the GRP and to press the cilia against the cell surface for measurement. *Xenopus* tissues were rehydrated, washed with PBS/0.1% TritonX-100 (PBT), and blocked with PBT containing 10% heat-inactivated normal goat serum (PBT/HIGS) for at least one hour. Zebrafish embryos were rehydrated in PBS/0.1% Tween-20 (PTW), and blocked in PTW + 5% HIGS + 2% Bovine Serum Albumin (BSA). Embryos were incubated with primary antibody in blocking solution overnight as follows: Rabbit anti-ZO-1 (Zymed 1:200), mouse monoclonal anti-acetylated tubulin (Sigma, 1:200-1:1000), monoclonal anti-gamma tubulin (Sigma, 1:1000), rabbit anti-GFP (Molecular Probes, 1:1000), or rabbit anti-dsRed (Clontech 1:1000). After washing, embryos were incubated overnight in Cy2, Cy3, or Cy5 labeled Goat anti-IgG of the appropriate species (all used at 1:500, Jackson ImmunoResearch), washed in PBT or PTW and then mounted in PVA/DABCO. Mounted embryos were imaged on a BioRad Radiance 2100 confocal mounted to a Zeiss inverted microscope using a 40× or 63× objective.

RNA Isolation and Microarray

Animal caps were explanted onto coverslips coated with fibronectin as described⁴⁰. Total RNA was isolated using the proteinase K method from explanted ectoderm at the equivalent of stage 22-24 of development. Total RNA from explanted ectoderm was used to generate labeled complimentary RNA (cRNA) that was hybridized to *Xenopus laevis* lGenome Array chips (Affymetrix #900491). Microarray data were obtained from three independent experiments in which embryos were injected with *ICD* RNA alone, and two independent experiments in which embryos were injected with both *ICD* and *FoxJ1* RNA. These data sets were analyzed using Bullfrog analysis software⁴¹ using a pair-wise comparison, with the minimum fold change set at 3. Data presented in Supplementary Table 1 show all genes

with an average change of 10-fold or greater. Annotation of the dataset was then performed using Unigene identifiers.

Quantitative RT-PCR

Total RNA was isolated at stage 22-24 from animal caps that had been explanted from stage 10 embryos onto fibronectin-coated coverslips as described above. cDNA templates were generated from 3µg of RNA using SuperScript III Reverse Transcriptase (Invitrogen). Quantitative RT-PCR reactions were performed using the ABI Prism 7900HT Thermal Cycler, using primers for cilia genes or for ornithine decarboxylase (ODC) as a normalization control (Supplementary Table 2). Data was analyzed using Applied Biosystems Sequence Detection System (SDS) software.

RT-PCR Analysis of Splicing Morpholino

Total RNA was harvested as for quantitative RT-PCR. PCR reactions were performed using a forward primer spanning the exon1-intron1 boundary (Splicing MO-F) and a reverse primer corresponding to the stop codon in the mRNA transcript (Splicing MO-R).

Wilson's Explants

Mesoderm cells were imaged by generating Wilson's explants in 100% Danilchik's in saline⁴² followed by fixation and immunostaining as listed above. Briefly, at stage 12, the endoderm and GRP were peeled away from the ventral side of a dorsal explant, thereby exposing the underlying mesoderm. Explants were kept in explant medium and held flat under a coverslip from stage 12 until stage 17/18 when they were fixed.

Zebrafish Strains

We used *mlc2a:eGFP* zebrafish strains for all experiments⁴³. Whole mount in-situ hybridizations were carried out as described⁴⁴. Zebrafish FoxJ1 (*ZFoxJ1*) antisense probes were generated from cDNA cloned using PCR from 2 day post fertilization (2dpf) total RNA. We designed an antisense morpholino targeted against the start codon *ZFoxJ1*^{MO} and a non-specific morpholino, ZControl (GeneTools, Supplementary Table 2). Embryos were injected with 3-5µg of morpholino. Heart jogging was assessed at 30-34hpf, by visualizing GFP expression in the heart.

High-speed microscopy

Albino *Xenopus* embryos were injected at the two-cell stage with *FoxJ1* and *ICD* RNA, targeting each blastomere twice on the animal pole. The ectoderm was explanted on the fibronectin-coated glass as above at stage 10, and cultured to the equivalent of stage 22 of development. Ectopic cilia were visualized under bright field illumination, and captured on an Olympus BX51 microscope using a 100× submersible objective and a Vision Research Phantom 7.2 (CMOS) camera at 20,000 fps.

Transmission Electron Microscopy

Embryos were fixed overnight at 4°C in 2% Glutaraldehyde, postfixed in OsO₄, stained with uranyl acetate, then embedded in EPON epoxy resin. Thin sections (60nm) were cut

and mounted on copper slot grids coated with parlodion, stained with uranyl acetate /lead citrate and imaged on a Philips CM100 electron microscope. Extensive use was made of the goniometer in conjunction with the rotation-tilt specimen holder and the orientation of the grids was adjusted up to ± 60 degree tilt to optimize as far as possible the cross sectional profile of the cilia. Images were documented using Kodak SO163 EM film that were scanned at 600 lpi using a Fuji FineScan 2750 \times 1 and converted to tif format.

Supplementary Material

Refer to Web version on PubMed Central for supplementary material.

Acknowledgments

The authors thank members of the Kintner lab for comments on the manuscript, Dr. Malcolm Wood for technical assistance with the TEM, and Dr. Brian Mitchell for assistance with high speed photography in collaboration with Drs Clare Yu, Peter Taborek, and Fawn Huisman in the Department of Physics at UC Irvine. The work was supported by NIH grants to CK, and JCB.

References

1. Satir P, Christensen ST. Overview of structure and function of mammalian cilia. *Annu Rev Physiol.* 2007; 69:377–400. [PubMed: 17009929]
2. Spektor A, Tsang WY, Khoo D, Dynlacht BD. Cep97 and CP110 suppress a cilia assembly program. *Cell.* 2007; 130:678–90. [PubMed: 17719545]
3. Whitsett JA, Tichelaar JW. Forkhead transcription factor HFH-4 and respiratory epithelial cell differentiation. *Am J Respir Cell Mol Biol.* 1999; 21:153–4. [PubMed: 10423395]
4. Hackett BP, et al. Primary structure of hepatocyte nuclear factor/forkhead homologue 4 and characterization of gene expression in the developing respiratory and reproductive epithelium. *Proc Natl Acad Sci U S A.* 1995; 92:4249–53. [PubMed: 7753791]
5. Pelletier GJ, Brody SL, Liapis H, White RA, Hackett BP. A human forkhead/winged-helix transcription factor expressed in developing pulmonary and renal epithelium. *Am J Physiol.* 1998; 274:L351–9. [PubMed: 9530170]
6. Lim L, Zhou H, Costa RH. The winged helix transcription factor HFH-4 is expressed during choroid plexus epithelial development in the mouse embryo. *Proc Natl Acad Sci U S A.* 1997; 94:3094–9. [PubMed: 9096351]
7. Huang T, et al. Foxj1 is required for apical localization of ezrin in airway epithelial cells. *J Cell Sci.* 2003; 116:4935–45. [PubMed: 14625387]
8. Gomperts BN, Gong-Cooper X, Hackett BP. Foxj1 regulates basal body anchoring to the cytoskeleton of ciliated pulmonary epithelial cells. *J Cell Sci.* 2004; 117:1329–37. [PubMed: 14996907]
9. Pan J, You Y, Huang T, Brody SL. RhoA-mediated apical actin enrichment is required for ciliogenesis and promoted by Foxj1. *J Cell Sci.* 2007; 120:1868–76. [PubMed: 17488776]
10. Chen J, Knowles HJ, Hebert JL, Hackett BP. Mutation of the mouse hepatocyte nuclear factor/forkhead homologue 4 gene results in an absence of cilia and random left-right asymmetry. *J Clin Invest.* 1998; 102:1077–82. [PubMed: 9739041]
11. Brody SL, Yan XH, Wuerffel MK, Song SK, Shapiro SD. Ciliogenesis and left-right axis defects in forkhead factor HFH-4-null mice. *Am J Respir Cell Mol Biol.* 2000; 23:45–51. [PubMed: 10873152]
12. Hirokawa N, Tanaka Y, Okada Y, Takeda S. Nodal flow and the generation of left-right asymmetry. *Cell.* 2006; 125:33–45. [PubMed: 16615888]
13. Nonaka S, et al. Randomization of left-right asymmetry due to loss of nodal cilia generating leftward flow of extraembryonic fluid in mice lacking KIF3B motor protein. *Cell.* 1998; 95:829–37. [PubMed: 9865700]

14. Takeda S, et al. Left-right asymmetry and kinesin superfamily protein KIF3A: new insights in determination of laterality and mesoderm induction by *kif3A*^{-/-} mice analysis. *J Cell Biol.* 1999; 145:825–36. [PubMed: 10330409]
15. Zhang M, Bolting MF, Knowles HJ, Karnes H, Hackett BP. *Foxj1* regulates asymmetric gene expression during left-right axis patterning in mice. *Biochem Biophys Res Commun.* 2004; 324:1413–20. [PubMed: 15504371]
16. Schweickert A, et al. Cilia-driven leftward flow determines laterality in *Xenopus*. *Curr Biol.* 2007; 17:60–6. [PubMed: 17208188]
17. Essner JJ, Amack JD, Nyholm MK, Harris EB, Yost HJ. Kupffer's vesicle is a ciliated organ of asymmetry in the zebrafish embryo that initiates left-right development of the brain, heart and gut. *Development.* 2005; 132:1247–60. [PubMed: 15716348]
18. Essner JJ, et al. Conserved function for embryonic nodal cilia. *Nature.* 2002; 418:37–8. [PubMed: 12097899]
19. Kramer-Zucker AG, et al. Cilia-driven fluid flow in the zebrafish pronephros, brain and Kupffer's vesicle is required for normal organogenesis. *Development.* 2005; 132:1907–21. [PubMed: 15790966]
20. Pohl BS, Knochel W. Isolation and developmental expression of *Xenopus* FoxJ1 and FoxK1. *Dev Genes Evol.* 2004; 214:200–5. [PubMed: 14986136]
21. Stubbs JL, Davidson L, Keller R, Kintner C. Radial intercalation of ciliated cells during *Xenopus* skin development. *Development.* 2006; 133:2507–15. [PubMed: 16728476]
22. Mitchell B, Jacobs R, Li J, Chien S, Kintner C. A positive feedback mechanism governs the polarity and motion of motile cilia. *Nature.* 2007; 447:97–101. [PubMed: 17450123]
23. Park TJ, Haigo SL, Wallingford JB. Ciliogenesis defects in embryos lacking inturned or fuzzy function are associated with failure of planar cell polarity and Hedgehog signaling. *Nat Genet.* 2006; 38:303–11. [PubMed: 16493421]
24. You Y, et al. Role of f-box factor *foxj1* in differentiation of ciliated airway epithelial cells. *Am J Physiol Lung Cell Mol Physiol.* 2004; 286:L650–7. [PubMed: 12818891]
25. Deblandre GA, Wettstein DA, Koyano-Nakagawa N, Kintner C. A two-step mechanism generates the spacing pattern of the ciliated cells in the skin of *Xenopus* embryos. *Development.* 1999; 126:4715–28. [PubMed: 10518489]
26. Liu Y, Pathak N, Kramer-Zucker A, Drummond IA. Notch signaling controls the differentiation of transporting epithelia and multiciliated cells in the zebrafish pronephros. *Development.* 2007; 134:1111–22. [PubMed: 17287248]
27. Ma M, Jiang YJ. Jagged2a-notch signaling mediates cell fate choice in the zebrafish pronephric duct. *PLoS Genet.* 2007; 3:e18. [PubMed: 17257056]
28. Feistel K, Blum M. Three types of cilia including a novel 9+4 axoneme on the notochordal plate of the rabbit embryo. *Dev Dyn.* 2006; 235:3348–58. [PubMed: 17061268]
29. Inglis PN, Boroevich KA, Leroux MR. Piecing together a ciliome. *Trends Genet.* 2006; 22:491–500. [PubMed: 16860433]
30. Sapiro R, et al. Male infertility, impaired sperm motility, and hydrocephalus in mice deficient in sperm-associated antigen 6. *Mol Cell Biol.* 2002; 22:6298–305. [PubMed: 12167721]
31. Tanaka H, et al. Mice deficient in the axonemal protein Tektin-t exhibit male infertility and immotile-cilium syndrome due to impaired inner arm dynein function. *Mol Cell Biol.* 2004; 24:7958–64. [PubMed: 15340058]
32. Supp DM, Potter SS, Brueckner M. Molecular motors: the driving force behind mammalian left-right development. *Trends Cell Biol.* 2000; 10:41–5. [PubMed: 10652513]
33. McGrath J, Somlo S, Makova S, Tian X, Brueckner M. Two populations of node monocilia initiate left-right asymmetry in the mouse. *Cell.* 2003; 114:61–73. [PubMed: 12859898]
34. Marshall WF, Kintner C. Cilia orientation and the fluid mechanics of development. *Curr Opin Cell Biol.* 2008; 20:48–52. [PubMed: 18194854]
35. Sive, H.; Grainger, RM.; Harland, RM. The early development of *Xenopus laevis*: a laboratory manual. Cold Spring Harbor Press; Plainview, NY: 1998.

36. Wettstein DA, Turner DL, Kintner C. The *Xenopus* homolog of *Drosophila* Suppressor of Hairless mediates Notch signaling during primary neurogenesis. *Development*. 1997; 124:693–702. [PubMed: 9043084]
37. Nasevicius A, Ekker SC. Effective targeted gene 'knockdown' in zebrafish. *Nat Genet*. 2000; 26:216–20. [PubMed: 11017081]
38. Heasman J. Morpholino oligos: making sense of antisense? *Dev Biol*. 2002; 243:209–14. [PubMed: 11884031]
39. Harland RM. In situ hybridization: an improved whole-mount method for *Xenopus* embryos. *Methods Cell Biol*. 1991; 36:685–95. [PubMed: 1811161]
40. Davidson LA, Hoffstrom BG, Keller R, DeSimone DW. Mesendoderm extension and mantle closure in *Xenopus laevis* gastrulation: combined roles for integrin alpha(5)beta(1), fibronectin, and tissue geometry. *Dev Biol*. 2002; 242:109–29. [PubMed: 11820810]
41. Zapala MA, Lockhart DJ, Pankratz DG, Garcia AJ, Barlow C. Software and methods for oligonucleotide and cDNA array data analysis. *Genome Biol*. 2002; 3:SOFTWARE0001. [PubMed: 12093384]
42. Wilson PA, Oster G, Keller R. Cell rearrangement and segmentation in *Xenopus*: direct observation of cultured explants. *Development*. 1989; 105:155–66. [PubMed: 2806114]
43. Huang CJ, Tu CT, Hsiao CD, Hsieh FJ, Tsai HJ. Germ-line transmission of a myocardium-specific GFP transgene reveals critical regulatory elements in the cardiac myosin light chain 2 promoter of zebrafish. *Dev Dyn*. 2003; 228:30–40. [PubMed: 12950077]
44. Thisse C, Thisse B, Schilling TF, Postlethwait JH. Structure of the zebrafish *snail1* gene and its expression in wild-type, spadetail and no tail mutant embryos. *Development*. 1993; 119:1203–15. [PubMed: 8306883]

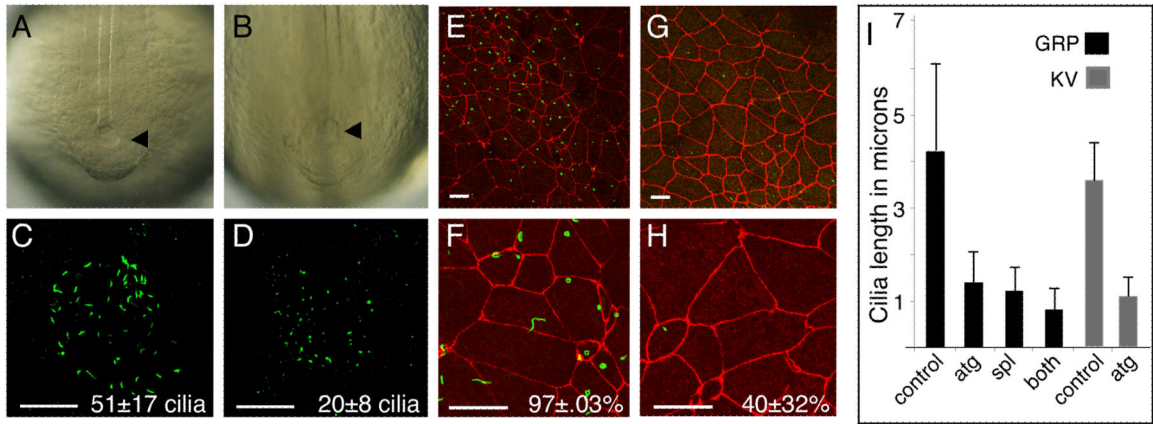


Figure 1.

Knock down of FoxJ1 activity inhibits ciliogenesis in the Zebrafish KV and *Xenopus* GRP. (A-B) KV (arrowhead) morphology was visualized in Zebrafish embryos using light field microscopy in control (A) *ZFoxJ1* morphants (B). (C-D) Cilia in KV were visualized by staining with the acetylated tubulin antibody (green) and confocal microscopy in control (C) and *ZFoxJ1* morphants (D). Average number of cilia per KV (n=12) is indicated (N±S.D.) (E-H) Dorsal explants were generated from stage 17 *Xenopus* embryos injected with a mixture of *XFoxJ1*-MO^{ATG} and *XFoxJ1*-MO^{SPL} (G,H) or with a control morpholino (E,F) and stained with ZO-1 (red) and acetylated tubulin (green) antibodies, to label cell junctions and cilia, respectively. The percentage of GRP cells (n=100-120 cells from 6 embryos) that extend cilia is indicated (%ciliated ±S.D.) Scale bars=20µm in all panels. (I) Cilia length (n=100-120 cilia from 6 embryos) was measured on the GRP of *Xenopus* embryos injected with a control-MO (control), with *XFoxJ1*-MO^{atg} (atg), with *XFoxJ1*-MO^{SPL} (spl), or with a mixture of both *XFoxJ1*-MOs (both). Cilia length in the KV of Zebrafish embryos (n=20 cilia from each of 6 embryos) injected with the *ZFoxJ1*-MO (atg) or with the control-MO (control). Error bars=S.D.

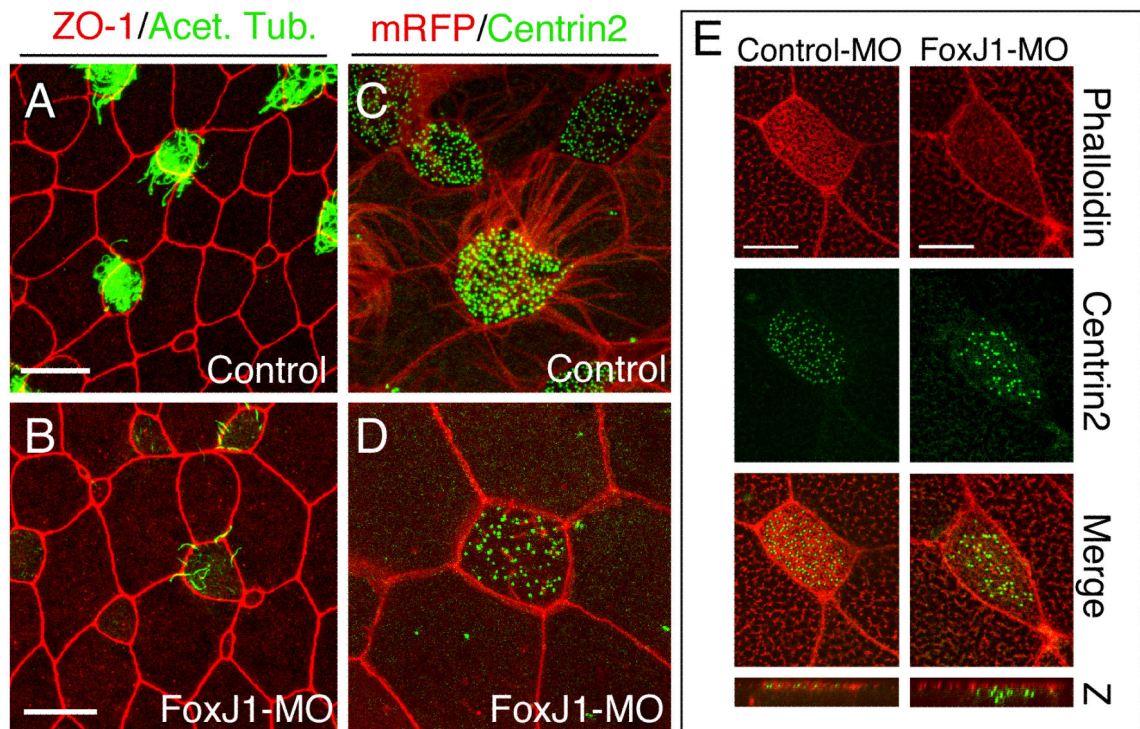


Figure 2.

XFoxJ1 morpholinos inhibits ciliogenesis in *Xenopus* skin cells.

(A-D) *Xenopus* embryos injected with both XFoxJ1 morpholinos, or a control morpholino were stained at stage 26 with ZO-1 (red) and anti-acetylated tubulin (green) to label cell borders and cilia, respectively (A,B), or were injected with RNAs encoding a membrane-localized RFP (red) and a GFP-centrin2 fusion protein (green), to label cell membranes and basal bodies, respectively (C,D). (E) Control or FoxJ1 morphants as above were co-injected with RNA encoding a GFP-centrin2 fusion protein (green), fixed at stage 26 and stained with rhodamine-phalloidin (red) to label the apical actin network. Bottom panels show a 2 μ m Z-scan through the apical domain. Scale bars represent 20 μ m in A-B and 10 μ m in C-E.

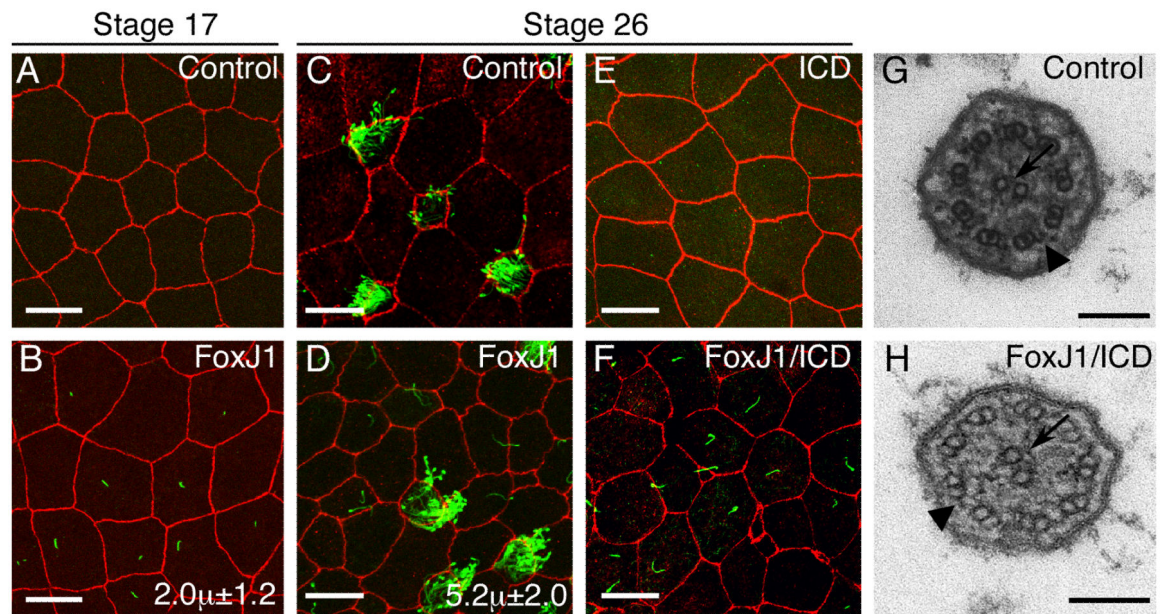


Figure 3.

XFoxJ1 RNA misexpression in surface epithelial cells induces ectopic cilia formation.

(A-F) Shown is a confocal image of the superficial epithelium in *Xenopus* embryos at the indicated stage, stained with antibodies to ZO-1 (Red) and acetylated-tubulin (green) to label cell borders and cilia, respectively. Embryos were injected at the two-cell stage with *RFP* RNA alone (A,C) with *FoxJ1* and *RFP* RNA (B,D), with *ICD* and *RFP* RNA (E) or with *FoxJ1*, *ICD* and *RFP* RNA (F). Average cilia length in microns is indicated in B and D (n=15-20 cilia from 3 embryos). Scale bars are 20µm. (G,H) Transmission electron micrographs of a cilium in a multi-ciliate cell (G) or of an ectopic cilium (H) induced by *FoxJ1* RNA in an ICD background (as in panel F). Arrows indicate the central pair and arrowheads indicate outer dynein arms. Scale bars are 100nm.

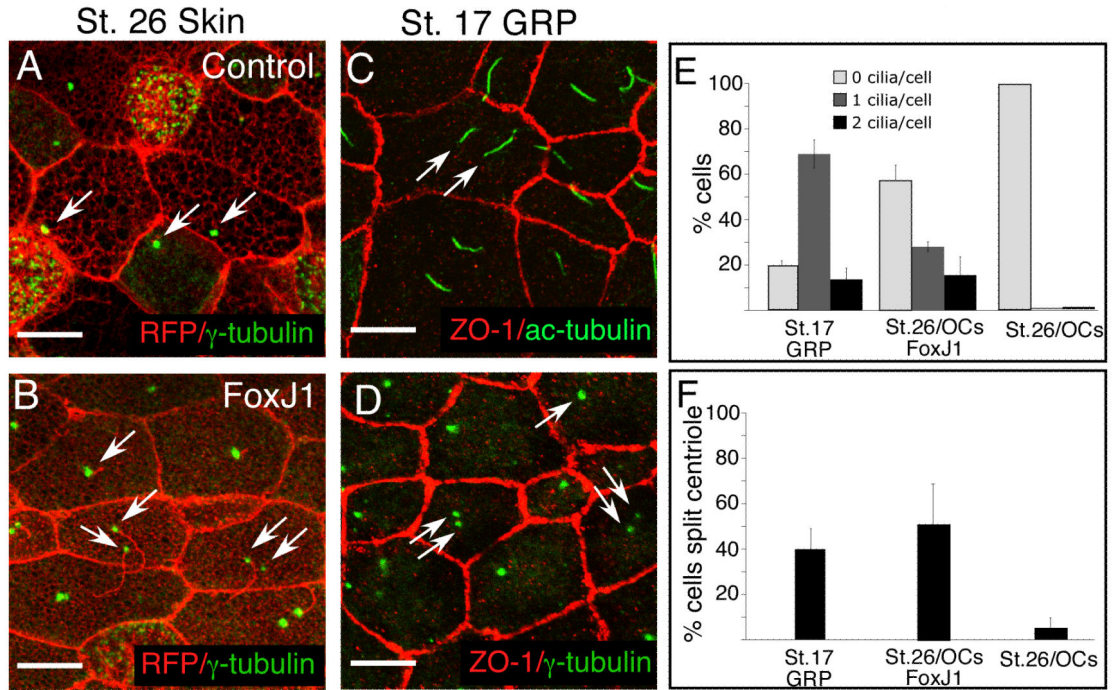


Figure 4. Bi-ciliate cells on the GRP and induced ectopically by XFoxJ1
(A-B) Shown is a confocal image of the skin at stage 26 of embryos injected with *RFP* RNA (A) or with both *FoxJ1* and *RFP* RNA (B), and stained with an antibody to γ -tubulin (green). Arrows denote centriole number and position. **(C-D)** Confocal image of the uninjected GRP at stage 17, either (C) stained with antibodies to ZO-1 (Red) and acetylated-tubulin (green) or (D) with antibodies to ZO-1 (Red) and γ -tubulin (green). Arrows indicate cilia number (C) or centriole position (D). Scale bars = 10 μ m. **(E-F)** Quantification of cilia number (E) and split centrioles (F) in the uninjected GRP at stage 17 (St.17 GRP, n=100 cilia or centriole pairs from each of 4 embryos), or in the outer epithelial cells (OCs) of stage 26 embryos that were injected with *FoxJ1* RNA (St26/OCs/*FoxJ1*) or with just *RFP* RNA as a control (St26/OCs). For stage 26 n=200 cilia or centriole pairs from each of 4 embryos. Error bars represent S.D.

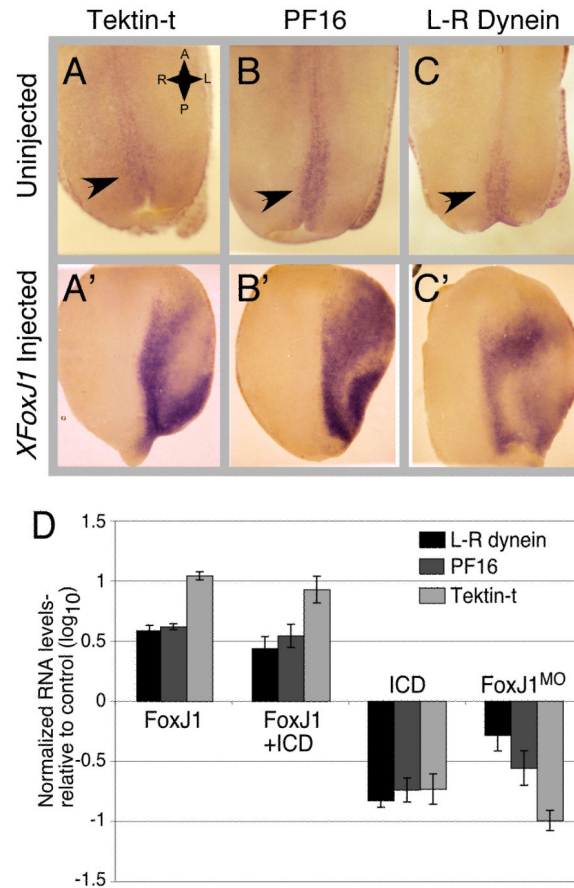


Figure 5.

Validation of gene expression regulated by *FoxJ1*.

(A-C) Shown is the roof of the gastrocoel in stage 17 embryos after staining for the expression of *Tektin-t* (A,A'), *PF16* (B,B') and *L-R dynein* (C,C') RNA using whole-mount, in situ hybridization. Expression (Red-Blue stain) in the posterior GRP is marked with an arrow. Top panels show staining in uninjected embryos while lower panels shows that in embryos injected twice in one blastomere at the two-cell stage with *XFoxJ1* RNA. Injected side is oriented to the right. (D) Embryos were injected at the two-cell stage with the indicated RNAs or with *XFoxJ1* or control morpholinos. At stage 10, the ectoderm was isolated, cultured on fibronectin-coated glass to stage 22, and then extracted for total RNA. The levels of *Tektin-t*, *PF16* (*Spag6*), or *L-R dynein* RNA was measured in each sample using quantitative PCR, and normalized relative to a ubiquitously expressed control RNA, *ODC*. Values for each experimental condition is an average of three measurements, and are expressed on a logarithmic plot as a ratio to the average value obtained with a control. Uninjected controls were used for the RNA injected samples and a control morpholino sample was used as a control for *FoxJ1* morpholino injection.

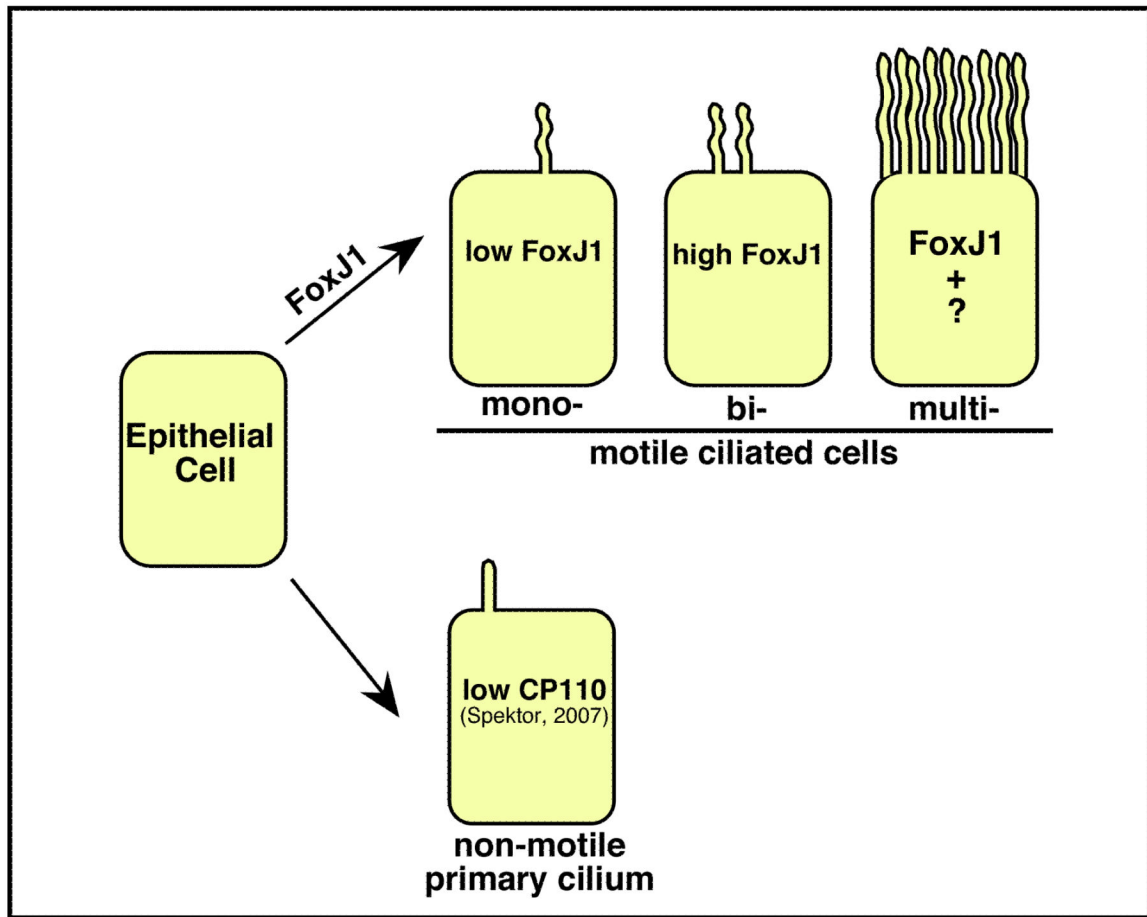


Figure 6. Model for cilia subtype specification. Epithelial cells (EC) extend non-motile primary cilia via a default pathway². In response to low levels of FoxJ1 epithelial cells extend a motile monocilia that can mediate flow required for left-right patterning. With increased levels of FoxJ1, ECs can be induced to form bi-ciliate cells. FoxJ1 also regulates the expression of genes required for the formation of motile cilia in multiciliated cells, whose differentiation requires additional unknown factor(s).